




In vitro synergistic antiviral activity of repurposed drugs against enterovirus 71

Kunlakanya Jitobaom¹ · Chompunuch Boonarkart¹ · Songkran Thongon¹ · Thanyaporn Sirihongthong¹ · Arpakorn Sornwong² · Prasert Auewarakul¹ · Ornpreeya Suptawiwat^{2,3} 

Received: 10 January 2024 / Accepted: 13 June 2024 / Published online: 30 July 2024
© The Author(s), under exclusive licence to Springer-Verlag GmbH Austria, part of Springer Nature 2024

Abstract

Enteroviruses cause viral diseases that are harmful to children. Hand, foot, and mouth disease (HFMD) with neurological complications is mainly caused by enterovirus 71 (EV71). Despite its clinical importance, there is no effective antiviral drug against EV71. However, several repurposed drugs have been shown to have antiviral activity against related viruses. Treatments with single drugs and two-drug combinations were performed *in vitro* to assess anti-EV71 activity. Three repurposed drug candidates with broad-spectrum antiviral activity were found to demonstrate potent anti-EV71 activity: prochlorperazine, niclosamide, and itraconazole. To improve antiviral activity, combinations of two drugs were tested. Niclosamide and itraconazole showed synergistic antiviral activity in Vero cells, whereas combinations of niclosamide-prochlorperazine and itraconazole-prochlorperazine showed only additive effects. Furthermore, the combination of itraconazole and prochlorperazine showed an additive effect in neuroblastoma cells. Itraconazole and prochlorperazine exert their antiviral activities by inhibiting Akt phosphorylation. Repurposing of drugs can provide a treatment solution for HFMD, and our data suggest that combining these drugs can enhance that efficacy.

Introduction

Enterovirus 71 (EV71) is a single-stranded, positive-sense, single-stranded RNA virus that belongs to the species *Enterovirus alphacoxsackie* of the family *Picornaviridae*. Coxsackieviruses A16 (CV-A16), CV-A6, and EV71 are the most common causative pathogens causing hand, foot, and mouth disease (HFMD) in infants and children younger than five years of age [52]. However, different viruses and subgenotypes predominate in different areas [5, 7, 22, 57]. The clinical presentation ranges from asymptomatic infection to mild HFMD, including fever, skin eruptions on the

hands and feet, and vesicles in the mouth. However, EV71 infection has also been implicated in causing severe neurological complications, including meningitis, encephalitis, acute flaccid paralysis, cardiopulmonary failure, and even death [29, 68]. EV71 is a highly transmissible virus. Transmission of the virus from person to person occurs by direct contact with secretions such as saliva, fluid from blisters, or via the fecal-oral route. EV71 was first isolated from patients with neurological disease in California in 1969. Recently, outbreaks of EV71 infection have occurred periodically worldwide, particularly in the Asia-Pacific region [44]. According to a recent study conducted in Bangkok, Thailand, EV71 is the most common virus causing HFMD in kindergartens [57].

To date, three inactivated EV71 vaccines have been licensed in China, and several multivalent vaccines are under development [30]. However, there are no specific antiviral agents for EV71 treatment; only supportive therapy is used as the primary treatment in severe cases. Although several antiviral agents and small compounds, including lactoferrin, pleconaril, and rupintrivir, have been reported to have an inhibitory effect against EV71, none of them has been shown to be clinically efficacious [28, 34, 60, 73, 74].

Communicated by Akbar Dastjerdi

✉ Ornpreeya Suptawiwat
ornpreya.sup@era.ac.th

¹ Department of Microbiology, Faculty of Medicine Siriraj Hospital, Mahidol University, Bangkok 10700, Thailand

² Department of Central instrument and Research Laboratory, Virology and Immunology Laboratory, Chulabhorn Royal Academy, Bangkok 10210, Thailand

³ Princess Srisavangavadhana College of Medicine, Chulabhorn Royal Academy, Bangkok 10210, Thailand

Therefore, the development of effective antiviral agents targeting EV71 is still needed.

The use of repurposed drugs is an attractive antiviral strategy because their safety profiles are already available [16]. Several FDA-approved drugs with broad-spectrum antiviral activity have been selected to evaluate their inhibitory effect against EV71. In particular, drugs that showed inhibitory effects on positive-sense RNA viruses, including flaviviruses, togaviruses, and coronaviruses, can also inhibit EV71, which is also a positive-sense RNA virus [16, 31]. In this study, the anti-EV71 activity of several FDA-approved drugs was evaluated *in vitro*. Furthermore, to improve antiviral activity and possible efficacy, a drug combination approach was evaluated. Combining different drugs has been a successful strategy for the treatment of various viral infections, such as hepatitis C virus (HCV) and human immunodeficiency virus 1 (HIV-1) infections [1, 43, 62].

Materials and methods

Chemicals

Niclosamide (N3510, Sigma), nitazoxanide (N0290, Sigma), temsirolimus (PZ0020, Sigma), prochlorperazine (P9178, Sigma), itraconazole (I6657, Sigma), mycophenolic acid (M3536, Sigma), sofosbuvir (HY-15005, MCE), 2,4-dinitrophenol (34334, Sigma), paromomycin (P5057, Sigma), and triparanol (T5200, Sigma) were dissolved in dimethyl sulfoxide (DMSO; Sigma) to make stock solutions with a concentration of 10 mM. Metformin (HY-17471A, MCE) was dissolved in water at a concentration of 10 mM. All stock solutions were stored at -80°C .

Immediately before use, the stock solutions were diluted to their working concentrations in culture medium containing 2% fetal bovine serum (FBS) (2% FBS-MEM or 2% FBS-DMEM/F12 + Opti-MEM). The final concentration of DMSO in all experiments was 0.1%.

Cells and viruses

Vero cells (CCL-81, ATCC) were maintained in minimum essential medium (MEM; Gibco) supplemented with 10% heat-inactivated FBS (MEM-10%FBS) at 37°C with 5% CO_2 . The human neuroblastoma cell line SH-SY5Y (CRL-2266, ATCC) was maintained in Dulbecco's modified Eagle medium/nutrient mixture F-12 (DMEM/F-12; 11320033, Gibco) and Opti-MEM reduced serum medium (11058021, Gibco) in a 1:1 ratio supplemented with 10% heat-inactivated fetal bovine serum (FBS, Gibco) at 37°C with 5% CO_2 . The EV71 subgenotype C4 strain used in this study was kindly provided by Prof. Pilaipan Puthavathana [38]

and propagated in Vero cells. Viral supernatants were harvested at 3 days postinfection, centrifuged to remove cell debris, and stored at -80°C . The virus titer of the stock virus was determined in Vero cells, using a plaque assay.

Enterovirus 71 infection

On the day before the experiment, Vero and SH-SY5Y cells were seeded in 96-well plates at a density of 3×10^4 and 2.5×10^4 cells/well, respectively. The next day, the culture medium was replaced with 2% FBS medium containing EV71 subgenotype C4 strain at the indicated multiplicity of infection (MOI) or 2% FBS medium without virus for mock infection for 1 hour at 37°C with 5% CO_2 . After incubation, the inoculum was removed and the cells were further cultured in 2% FBS-MEM or 2% FBS-DMEM/F12 + opti-MEM for Vero and SH-SY5Y cells, respectively.

Cell viability assay

Vero and SH-SY5Y cells were seeded in 96-well plates at a density of 3×10^4 and 2.5×10^4 cells/well, respectively. The cells were then treated with twofold serially diluted drugs in 2% FBS medium for 48 hours. Cell viability was determined using PrestoBlue Cell Viability Reagent (Invitrogen). After adding the cell-permeable resazurin-based (nonfluorescent) reagent, the reducing environment in viable cells converts resazurin to resorufin, which emits a red fluorescent signal that is detectable with an excitation wavelength of 560 nm and an emission wavelength of 590 nm. Alternatively, MTT dyes (Invitrogen) were also used. Live cells convert 3-(4,5-dimethyl-2-thiazolyl)-2,5-diphenyl-2H-tetrazolium bromide to MTT formazan. MTT formazan can be detected by measuring absorbance at 570 nm after dissolving the sample in DMSO. Cells treated with 0.1% DMSO were used as untreated controls. GraphPad Prism 9 (GraphPad Software, Inc., CA) was used for non-linear regression analysis and determination of the 50% cytotoxic concentration (CC_{50}).

Viral quantification using a plaque assay

Before infection, Vero cells were seeded in 24-well plates at a density that allowed them to grow to 100% confluency within 24 hours. The next day, the cells were inoculated with a tenfold serial dilution of viral samples for 1 hour at 37°C with 5% CO_2 . After incubation, the inoculum was removed, and the cells were overlaid with 1.2% microcrystalline cellulose (Avicel, RC-591) in 2% FBS-MEM and incubated at 37°C and 5% CO_2 for three days. The overlaid Avicel was then removed, and the plates were fixed with 10% formalin (v/v) in phosphate-buffered saline (PBS) for 1–2 hours. The

plates were then rinsed with tap water and stained for 5 minutes with 1% crystal violet (w/v) in 20% (v/v) ethanol. The plaques were counted to calculate the viral titers in plaque-forming units per milliliter (pfu/ml).

Drug treatments

Anti-EV71 activity screening

Eleven FDA-approved drug candidates were selected based on a review of the literature. Vero cells were seeded at a density of 3×10^4 cells/well in 96-well plates. Cells were pretreated with each drug at a concentration of 10 μ M for 1 hour at 37°C with 5% CO₂. The treated cells were then inoculated with EV71 subgenotype C4 at an MOI of 0.01 for 1 hour. The supernatant was then removed, and the cells were maintained in the medium with the drug for two days. The antiviral effect was determined based on the observed cytopathic effect (CPE).

Dose-response curves of single drug treatment

Prior to the day of drug treatments, Vero and SH-SY5Y cells were seeded in 96-well plates at a density of 3×10^4 and 2.5×10^4 cells/well, respectively. Each drug was serially diluted twofold and incubated with the cells for 1 hour. Subsequently, Vero and SH-SY5Y cells were infected with EV71 subgenotype C4 at an MOI of 0.01 and 2, respectively, for 1 hour. The inoculation supernatant was then removed, and the cells were further cultured in the medium containing the serially diluted drugs for two days. The virus titers were determined using a plaque assay. The half-maximal inhibitory concentration (IC₅₀) was calculated from the dose-response curves.

Dose-response curves of two-drug combinations

Cells were pretreated with a series of serial twofold dilutions of the two-drug combinations for 1 hour at 37°C with 5% CO₂, followed by infection with EV71 as described above. At 2 days postinfection, virus supernatants were collected and virus titers were measured by plaque assay.

Evaluation of two-drug combination treatments

The day before the experiment, Vero and SH-SY5Y cells were seeded in 96-well plates at a density of 3×10^4 and 2.5×10^4 cells/well, respectively. The cells were then pretreated with 16 or 20 different pairwise combinations of two drugs for 1 hour. The concentrations of each drug were 2, 1, 0.5, 0.25, and 0.125 times its IC₅₀ value. Vero and SH-SY5Y cells were then infected for 1 hour with EV71 subgenotype

C4 at an MOI of 0.01 and 2, respectively. The virus inoculum was then removed, and the cells were cultured further in the presence of the drugs for two days. The virus titers were determined by plaque assay.

Analysis of the interaction between two drugs

Drug interaction was analyzed using the SynergyFinder web application (<https://synergyfinder.fimm.fi>). We used four different reference models: the Loewe additivity (Loewe), zero independence potency (ZIP), highest single agent (HSA), and Bliss independence models [67]. Synergy scores less than -10 indicated an antagonistic interaction, scores between -10 and 10 indicated an additive effect, and scores greater than 10 indicated a synergistic effect between two drugs. The synergy score for each pair is presented as the mean and confidence interval.

Western blot analysis

Infected cells were lysed in RIPA buffer (50 mM Tris-HCl pH 8.0, 150 mM NaCl, 0.1% Triton X-100, 0.5% sodium deoxycholate, 0.1% sodium dodecyl sulfate [SDS], 1 mM sodium orthovanadate, and 1 mM NaF). Cell debris was removed by centrifugation at 12,000 \times g for 10 min at 4°C. The cell lysate was then transferred to a new tube, and the protein concentration was measured by the Bradford method. The lysate was loaded onto a NuPAGE 10% Bis-Tris protein gel (1.0 mm) (NP0302BOX; Thermo Fisher Scientific), and after electrophoresis, the proteins were transferred to a nitrocellulose membrane (PALL) by diffusion blotting. The membrane was then blocked with 3% (w/v) skim milk in 0.1% Tween 20 (v/v)-TBS for 1 hour at room temperature and then probed with a 1:1000 dilution of rabbit anti-Akt (#9272), anti-phospho-Akt (#4060), anti-phospho mTOR (#2971), anti-mTOR (#2983), and anti-EV71 (MAB979, Millipore) or a 1:10,000 dilution of antibody against 3-phosphate dehydrogenase (GAPDH, sc-32233; Santa Cruz Biotechnology, Inc.) at 4°C overnight with continuous rocking. The membrane was washed and incubated with a 1:2000 dilution of horseradish peroxidase (HRP)-conjugated goat anti-rabbit IgG or HRP-conjugated rabbit anti-mouse IgG for 2 hours at room temperature. Protein bands were visualized by incubating the membrane with Clarity Western ECL substrate (Bio-Rad Laboratories, Hercules, CA, USA) and photographed using ImageQuant LAS 4010 (GE Healthcare, Chicago, IL, USA). The protein band intensities were determined using ImageJ software (U.S. National Institutes of Health, Bethesda, MD, USA) and normalized to the GAPDH expression level. The ratios of p-AKT/AKT and p-mTOR/mTOR were calculated based on the GAPDH-normalized expression level.

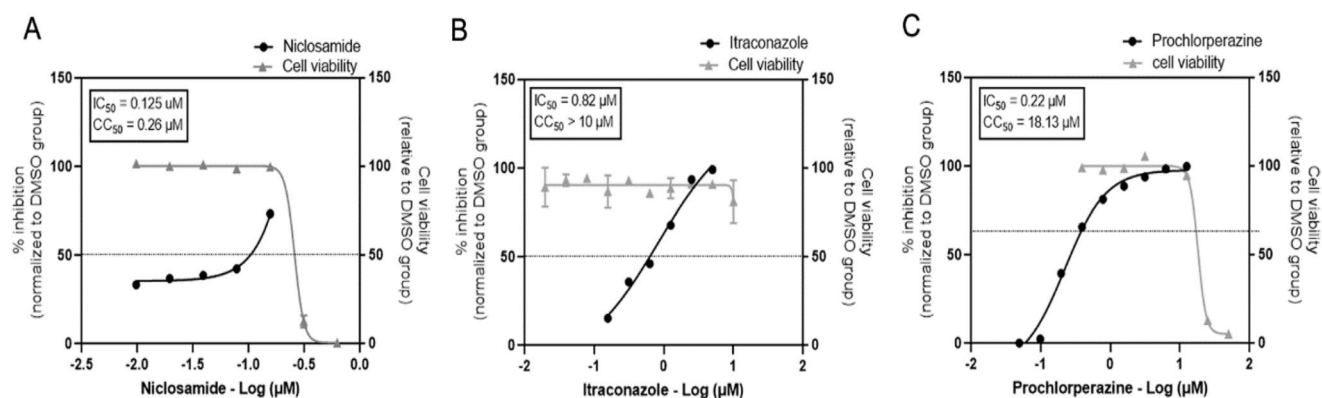


Fig. 1 Dose-response curves for single-drug treatment against EV71 subgenotype C4 in Vero cells. **(A)** niclosamide. **(B)** itraconazole. **(C)** prochlorperazine. Vero cells were pretreated with twofold serial dilutions of each drug for 1 hour and infected with EV71 at an MOI of 0.01. The infected cells were maintained for two days in medium containing serially diluted drugs or 0.1% DMSO without drugs. The

virus production was detected using a plaque assay. The dose-response curves are expressed as percent inhibition relative to 0.1% DMSO-treated cells. The effect of drug treatment on cell viability was assessed relative to 0.1% DMSO-treated cells using PrestoBlue reagent. The data are presented as the mean \pm standard deviation

Table 1 Single-drug treatment against EV71 subgenotype C4 in Vero and neuroblastoma cells (SH-SY5Y)

Drug treatment	Vero cells			SH-SY-5Y		
	CC ₅₀ (μM)	IC ₅₀ (μM)	Selectivity index (CC ₅₀ /IC ₅₀)	CC ₅₀ (μM)	IC ₅₀ (μM)	Selectivity index (CC ₅₀ /IC ₅₀)
Niclosamide	0.26	0.125	2.08	0.39	0.29	1.34
Itraconazole	> 10	0.82	> 12.20	> 10	0.41	> 24.39
Prochlorperazine	18.13	0.22	82.41	13.13	1.02	12.87

Statistical analysis

The experiments were carried out in triplicate. Percent inhibition and protein band intensity values are shown as the mean \pm SD. Comparisons between groups were made using an independent-sample *t*-test in SPSS Statistics software (SPSS, Inc., Chicago, IL, USA). A *p*-value ≤ 0.05 was considered statistically significant. Nonlinear regression analysis in GraphPad Prism 9 (GraphPad Software, Inc., CA) was used to determine IC₅₀ and CC₅₀ values.

Results

Antiviral activity of drug candidates against EV71 subgenotype C4 in Vero cells

FDA-approved drugs with antiviral activity were selected for the study of their antiviral activity against EV71. These included prochlorperazine [6, 17, 51], itraconazole [15, 53], niclosamide [23, 26, 33, 61, 64], nitazoxanide [20, 42, 46, 47, 50, 61], temsirolimus [13], mycophenolic acid [3, 10, 18], sofosbuvir [14, 48], metformin [8, 11, 45, 66], 2,4 dinitrophenol [55], paromomycin [19, 56], and triparanol [24].

The antiviral activity against EV71 of the selected drugs at a concentration of 10 μM was tested in Vero cells.

A compound was judged to have an inhibitory effect if it resulted in a decrease in the virus-induced cytopathic effect (CPE). Using a 50% CPE reduction threshold, significant antiviral activity was observed only for prochlorperazine and itraconazole. Niclosamide at a concentration of 10 μM was toxic to the cells; therefore, the CPE assay could not be used to determine its antiviral activity. Therefore, the antiviral activity of prochlorperazine, itraconazole, and niclosamide was tested at lower concentrations.

The cytotoxicity and antiviral activity of the three drug candidates against the EV71 subgenotype C4 in Vero cells are shown in Fig. 1 and Table 1. The IC₅₀ values for niclosamide, itraconazole, and prochlorperazine were 0.125, 0.82, and 0.22 μM, respectively. The CC₅₀ values for niclosamide, itraconazole, and prochlorperazine were 0.26, > 10, and 18.18 μM, respectively. Treatment with itraconazole and prochlorperazine yielded favorable selectivity index (SI) values of > 12.20 and 82.41, respectively (Table 1).

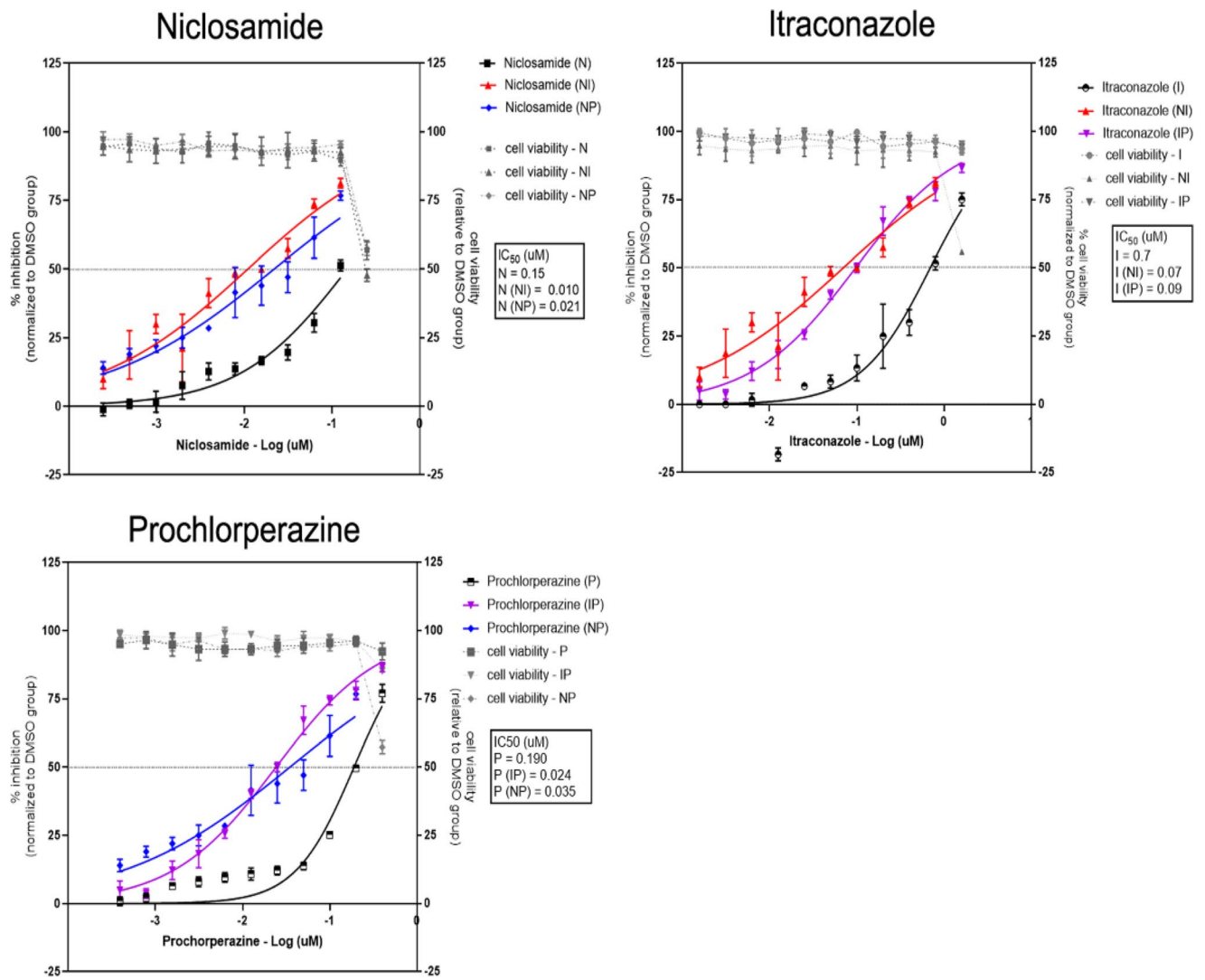


Fig. 2 Dose-response curves of two-drug combination treatment against EV71 subgenotype C4 in Vero cells. Vero cells were pre-treated either with twofold serial dilutions of single drugs or two-drug combinations for 1 hour and infected with EV71 subgenotype C4 at an MOI of 0.01. Then the cells were maintained for two days in medium containing serial dilutions of a single drug or a two-drug combination. Viral titers were determined using a plaque assay. The

dose-response curves are expressed as the percent inhibition relative to 0.1% DMSO-treated cells. The effect of drug treatment on cell viability was assessed relative to 0.1% DMSO-treated cells using an MTT assay. The two-drug combinations include niclosamide-itraconazole (NI), niclosamide-prochlorperazine (NP), and itraconazole-prochlorperazine (IP). The data are presented as the mean ± standard deviation. N, niclosamide; I, itraconazole; P, prochlorperazine

Table 2 Two-drug combination treatment against EV71 subgenotype C4 in Vero cells

Drug treatment	IC ₅₀ (μM)	Fold reduction of IC ₅₀ (single/combined)
Niclosamide	0.150	
Niclosamide + itraconazole	0.010	15
Niclosamide + prochlorperazine	0.021	7.14
Itraconazole	0.70	
Itraconazole + niclosamide	0.07	10
Itraconazole + prochlorperazine	0.09	7.78
Prochlorperazine	0.19	
Prochlorperazine + itraconazole	0.024	7.92
Prochlorperazine + niclosamide	0.035	5.43

Antiviral activity of two-drug combinations against EV71 subgenotype C4 in Vero cells

Dose-response curves of two-drug combinations

The dose-response curves of two-drug combination treatments and the IC₅₀ values are shown in Fig. 2 and Table 2. In combination with itraconazole or prochlorperazine, the dose-response curve of niclosamide was shifted, resulting in a 15- and 7.14-fold reduction, respectively, in the IC₅₀ value for niclosamide. The dose-response curve was also altered by the addition of niclosamide or prochlorperazine,

with a 10- and 7.78-fold reduction, respectively, in the IC_{50} value of itraconazole. The dose-response curve of prochlorperazine was also altered by adding niclosamide or itraconazole. The IC_{50} value of prochlorperazine was reduced by 7.92- and 5.43-fold, respectively. The combinations of niclosamide-itraconazole and itraconazole-prochlorperazine showed a stronger antiviral effect than the combination of niclosamide-prochlorperazine.

Evaluation of two-drug combination treatment against EV71 subgenotype C4 in Vero cells

To identify drug combinations with high potential for EV71 treatment, the antiviral effects of two-drug combinations were investigated in Vero cells following the same infection methodology with each pairwise combination.

Niclosamide-itraconazole combination

The dose-response curve for niclosamide showed a strong shift in the presence of itraconazole (Fig. 3A). A similar change in the dose-response curve of itraconazole was also observed in the presence of niclosamide (Fig. 3B). The dose-response matrix shows the relationship between increasing inhibitory activity and increased concentrations of both drugs (Fig. 3C). The interaction between the two drugs was analyzed, and a mean Loewe synergy score of 12.01 was obtained, indicating a synergistic effect (score greater than 10), with a peak score of 24.29 (95% confidence interval, CI 10.68, 29.44) for the mixture of 0.2 μ M itraconazole and 0.0625 μ M niclosamide (Fig. 3D and E). Using other reference models, including ZIP, HSA, and Bliss independence, mean synergy scores of 12.89, 22.68, and 12.96, respectively, were obtained, confirming the synergistic effect between niclosamide and itraconazole. There was no significant cytotoxicity in any of the pairwise combinations (Fig. 3A and B).

Niclosamide-prochlorperazine combination

Prochlorperazine at 0.4 μ M caused a strong shift in the dose-response curve of niclosamide. Furthermore, prochlorperazine at concentrations of 0.2, 0.1, 0.05, and 0.025 μ M decreased the IC_{50} value of niclosamide 5.67, 3.67, 1.86, and 1.44 times, respectively (Fig. 4A). The prochlorperazine dose-response curve also underwent a strong shift in the presence of 0.125 μ M niclosamide. The IC_{50} value of prochlorperazine was decreased 3 and 1.29 times in the presence of 0.0625 and 0.03125 μ M niclosamide, respectively (Fig. 4B). However, the dose-response curve of prochlorperazine was not affected by the presence of 0.015625 μ M niclosamide. Only pairwise combinations containing high

concentrations of both drugs showed an obvious increase in inhibitory activity (Fig. 4C). A mean Loewe synergy score of 3.25 indicated an additive effect (score greater than -10 and less than 10) between niclosamide and prochlorperazine, with a maximum score of 26.71 [23.65, 30.48] (Fig. 4D and E). The mean synergy scores calculated by ZIP, HSA, and Bliss independence were -7.02, 5.04, and -8.61, respectively, which also indicated an additive effect between niclosamide and prochlorperazine. There was no significant cytotoxicity in any of the pairwise combinations (Fig. 3A and B).

Itraconazole-prochlorperazine combination

The dose-response curve of itraconazole was strongly shifted by the addition of 0.4 μ M prochlorperazine. Prochlorperazine at concentrations of 0.2 and 0.1 μ M decreased the IC_{50} value of itraconazole by 2.84 and 1.64 times, respectively. However, the presence of 0.05 and 0.0025 μ M prochlorperazine caused a smaller effect (Fig. 5A). In a similar pattern, the dose-response curves of prochlorperazine were strongly shifted by the presence of 0.8 μ M itraconazole, and the IC_{50} value of prochlorperazine was decreased 7.95 and 2.90-fold by 0.4 and 0.2 μ M itraconazole, respectively. The presence of 0.1 μ M itraconazole did not cause a change in the IC_{50} value of prochlorperazine (Fig. 5B). Pairwise combinations with high concentrations of both drugs exhibited significant inhibitory effects (Fig. 5C). The mean Loewe synergy score of 3.77 indicated an additive effect (score greater than -10 and less than 10) between itraconazole and prochlorperazine, with a peak score of 28.84 [20.54, 31.80] at the maximum concentration of both drugs (Fig. 5D and E). The mean synergy scores obtained using the ZIP and Bliss independence models were 1.47 and 1.41, respectively, which also indicated an additive effect of itraconazole and prochlorperazine. The HSA model yielded a mean synergy score of 10.3, suggesting a possible synergistic effect. There was no significant cytotoxicity in any of the pairwise combinations (Fig. 3A and B).

Antiviral activity of drug candidates against EV71 subgenotype C4 in neuroblastoma cells

The antiviral activity of repurposed drug candidates against EV71 was examined in human neuroblastoma cells (SH-SY5Y), since this virus can cause a number of serious neurological complications. The cytotoxicity and antiviral activity of niclosamide, itraconazole, and prochlorperazine against EV71 subgenotype C4 are shown in Table 1 and Fig. 6. The IC_{50} values for niclosamide, itraconazole, and prochlorperazine were 0.29, 0.41, and 1.02 μ M, respectively. The CC_{50} values for niclosamide, itraconazole, and

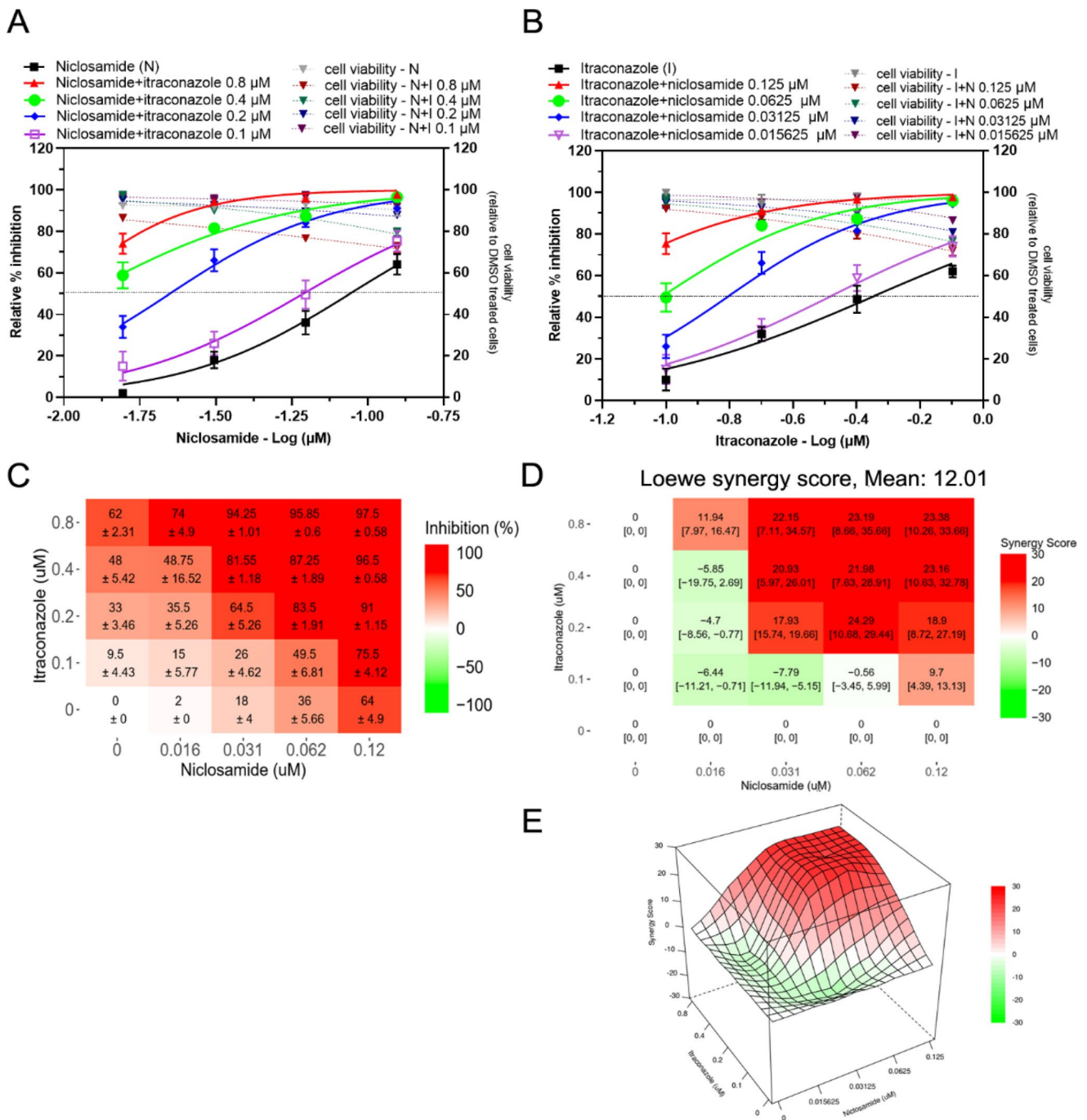


Fig. 3 Evaluation of the effect of niclosamide-itraconazole treatment on EV71 subgenotype C4 in Vero cells. Vero cells were pretreated for 1 hour with 16 different pairwise combinations of different concentrations of niclosamide and itraconazole. The cells were then infected with EV71 subgenotype C4 at an MOI of 0.01. After removing the inoculum, the cells were maintained for two days in the medium containing drugs. Virus titers were determined using a plaque assay. The percent inhibition relative to 0.1% DMSO-treated cells is shown in panel (A) for the treatment with twofold serial dilutions of niclosamide in the presence of different fixed concentrations of itraconazole and in panel (B) for the treatment with twofold serial dilutions of itraconazole

in the presence of different fixed concentrations of niclosamide. The dose-response matrix of each drug treatment is shown in panel (C). The data are presented as the mean ± standard deviation. The interaction between pairs of drugs was analyzed using SynergyFinder. The synergy score of each pairwise combination is represented by the mean and the confidence interval (D). The 3D synergy plot is shown in panel (E). A synergy scores less than -10 indicates antagonistic interaction between two drugs; a score between -10 and 10 indicates an additive effect of the two drugs; and a score greater than 10 indicates a synergistic effect of the two drugs. N, niclosamide; I, itraconazole

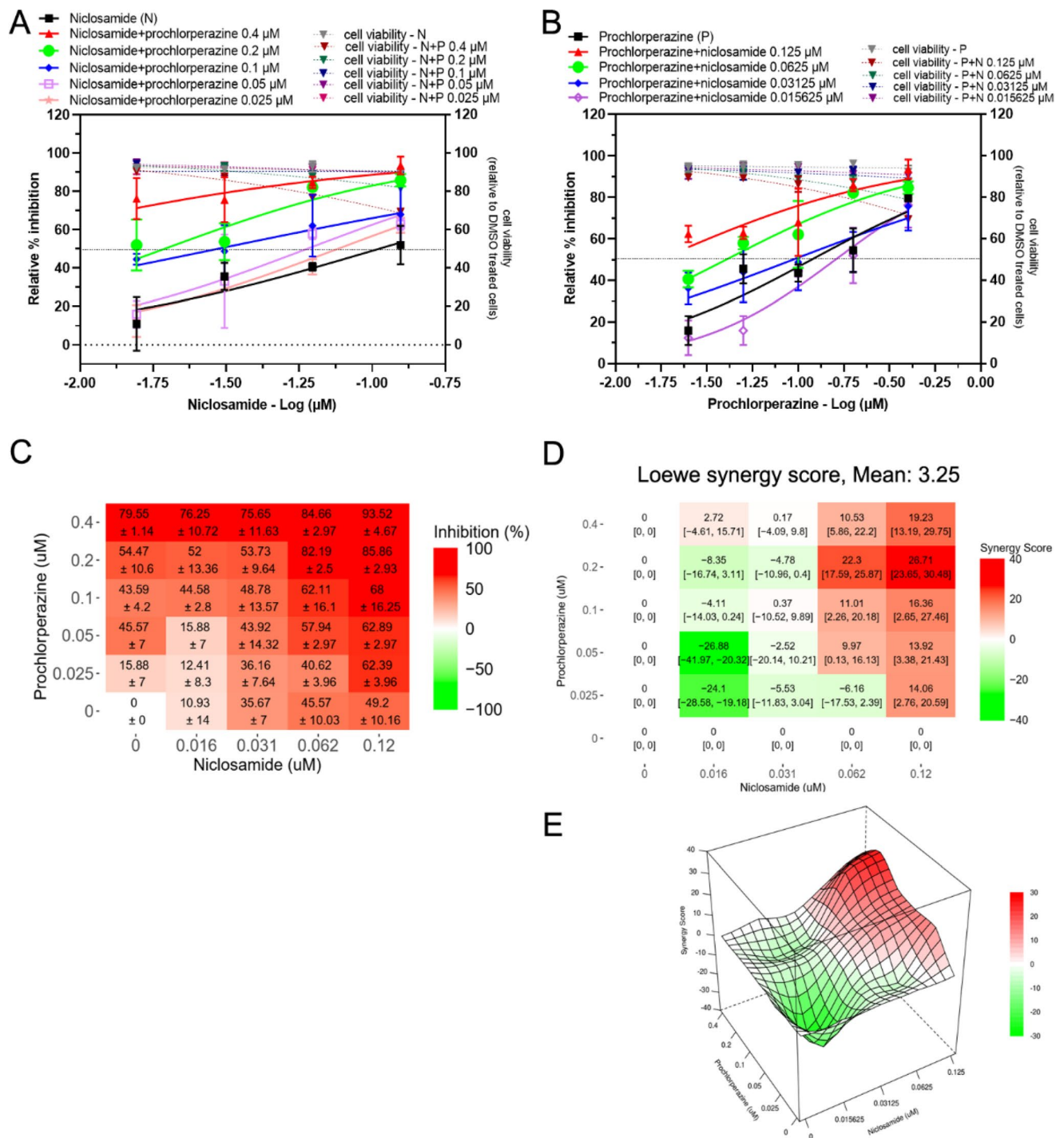


Fig. 4 Evaluation of the effect of niclosamide-prochlorperazine treatment on EV71 subgenotype C4 in Vero cells. Vero cells were pre-treated for 1 hour with 20 different pairwise combinations of different concentrations of niclosamide and prochlorperazine. The cells were then infected with EV71 subgenotype C4 at an MOI of 0.01. After removing the inoculum, the cells were maintained for two days in the medium containing drugs. Virus titers were determined using a plaque assay. The percent inhibition relative to 0.1% DMSO-treated cells is shown in panel (A) for the treatment with twofold serial dilutions of niclosamide in the presence of different fixed concentrations of prochlorperazine and in panel (B) for the treatment with twofold serial

dilutions of prochlorperazine in the presence of different fixed concentrations of niclosamide. The dose-response matrix of each drug treatment is shown in panel (C). The data are presented as the mean \pm standard deviation. The interaction between pairs of drugs was analyzed using SynergyFinder. The synergy score of each pairwise combination is presented as the mean and the confidence interval (D). A 3D synergy plot is shown in panel (E). A synergy scores less than -10 indicates an antagonistic interaction between the two drugs; a score between -10 and 10 indicates an additive effect of the two drugs; and a score greater than 10 indicates a synergistic effect of the two drugs. N, niclosamide; P, prochlorperazine

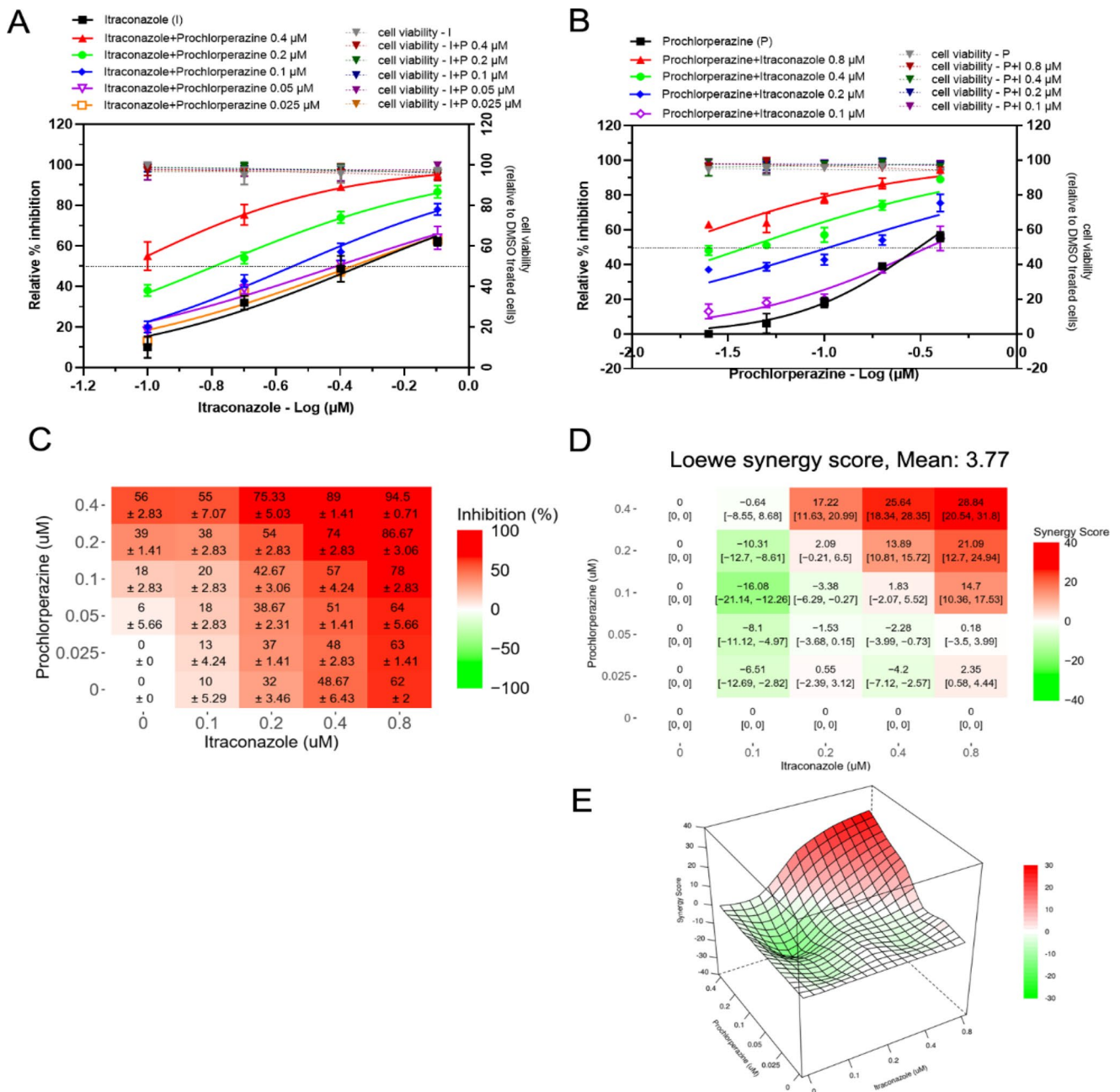


Fig. 5 Evaluation of the effect of itraconazole-prochlorperazine treatment on EV71 subgenotype C4 in Vero cells. Vero cells were pre-treated for 1 hour with 20 different pairwise combinations of different concentrations of itraconazole and prochlorperazine. The cells were then infected with EV71 subgenotype C4 at an MOI of 0.01. After removing the inoculum, the cells were maintained for two days in the medium containing drugs. Virus titers were determined using a plaque assay. The percent inhibition relative to 0.1% DMSO-treated cells is shown in panel (A) for the treatment with twofold serial dilutions of itraconazole in the presence of different fixed concentrations of prochlorperazine and in panel (B) for the treatment with twofold

serial dilutions of prochlorperazine in the presence of different fixed concentrations of itraconazole. The dose-response matrix for each drug treatment is shown in panel (C). The data are represented as the mean \pm standard deviation. The interaction between pairs of drugs was analyzed using SynergyFinder. The synergy score of each pairwise combination is presented as the mean and the confidence interval (D). A 3D synergy plot is shown in panel (E). A synergy score less than -10 indicates an antagonistic interaction between two drugs; a score between -10 and 10 indicates an additive effect of the two drugs; and a score greater than 10 indicates a synergistic effect of the two drugs. I, itraconazole; P, prochlorperazine

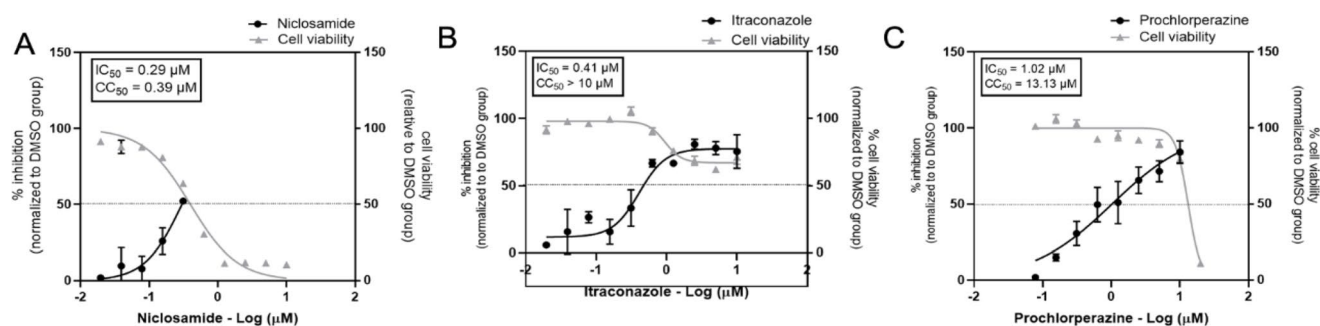


Fig. 6 Evaluation of antiviral activity of the drug candidates against EV71 subgenotype C4 in neuroblastoma cells. Dose-response curves for single-drug treatment against EV71 are shown. (A) niclosamide. (B) itraconazole. (C) prochlorperazine. The cells were treated with twofold serial dilutions of the drug for 1 hour and infected with EV71 subgenotype C4 at an MOI of 2. The infected cells were then main-

prochlorperazine were 0.39, > 10, and 13.13 μM , respectively. Niclosamide treatment resulted in an unfavorable selectivity index (SI) of 1.34. Treatment with itraconazole and prochlorperazine resulted in a more favorable SI of > 24.39 and 12.87, respectively.

Evaluation of two-drug combination treatment against EV71 in neuroblastoma cells

Itraconazole-prochlorperazine combination

Only the combination of itraconazole and prochlorperazine was tested in neuroblastoma cells due to their favorable SI. It was found that the presence of various concentrations of prochlorperazine induced a shift in the dose-response curve of itraconazole (Fig. 7A). The strongest inhibitory effect was observed with the combination of itraconazole and 0.2 μM prochlorperazine. Similarly, the presence of itraconazole induced a shift in the dose-response curve of prochlorperazine, with stronger inhibitory effects observed in the presence of 0.8, 0.4, and 0.1 μM itraconazole. However, the presence of 0.2 μM itraconazole gave an unusual result compared to the single drug treatment and the other combinations (Fig. 7B). The dose-response matrix demonstrated significant inhibitory activity in pairwise combinations of itraconazole and prochlorperazine (Fig. 7C). The mean Loewe synergy score of 7.68 indicates an additive effect (score greater than -10 and less than 10) between itraconazole and prochlorperazine, with a maximum score of 23.17 [19.6, 26.58] (Fig. 7D and E). When alternative reference models were used for the calculation of the synergy score, the HSA model yielded a synergy score of 9.02, indicating an additive effect. However, the synergy scores obtained using the ZIP and Bliss independence models were -12.47 and -10.86, respectively, indicating an antagonistic effect between itraconazole and prochlorperazine. There was no

tained for two days in the medium containing each drug or 0.1% DMSO as a control. Virus titers were determined using a plaque assay. The dose-response curves show the percent inhibition relative to 0.1%-DMSO-treated cells. The effect of drug treatment on cell viability relative to 0.1%-DMSO-treated cells was determined using PrestoBlue reagent. The data are shown as the mean \pm standard deviation

significant cytotoxicity in any of the pairwise combinations (Fig. 3A and B).

Inhibition of AKT phosphorylation by prochlorperazine and itraconazole

EV71 infection induces apoptosis, which limits viral replication [70]. However, previous studies have demonstrated that EV71 infection also activates PI3K/Akt signaling, which is the pathway that promotes cell survival and growth, in an early stage of infection to complete its replication cycle [70, 75]. Therefore, agents that inhibit PI3K/Akt signaling activation may result in inhibition of EV71.

Anticancer studies have shown that prochlorperazine and itraconazole inhibit Akt signaling [39, 58, 72]. Although these drugs are believed to inhibit viral replication through inhibition of endosomal acidification and cholesterol transport, respectively, inhibition of Akt signaling may also contribute to their antiviral effect. To investigate the effect of prochlorperazine and itraconazole on the PI3K/Akt signaling pathway, expression levels of the Akt protein were determined (Fig. 8). The results showed that EV71 infection activated the Akt signaling pathway by increasing phosphorylated Akt (p-Akt) in both Vero and neuroblastoma cells (Fig. 8A–D). Akt phosphorylation was reduced by treatment with prochlorperazine or itraconazole (Fig. 8B and D). One of the main cellular signaling pathways downstream of Akt is the mammalian rapamycin target (mTOR) pathway, which, upon activation, stimulates cell proliferation, protein synthesis, and *de novo* fatty acid synthesis, leading to an anti-apoptotic state that may favor viral replication [41, 71]. Therefore, mTOR activation was investigated in EV71-infected neuroblastoma cells. EV71 infection resulted in an increase in phosphorylated mTOR (p-mTOR) (Fig. 8C and E). Relatively lower expression of p-mTOR was observed in cells treated with prochlorperazine, and this correlated

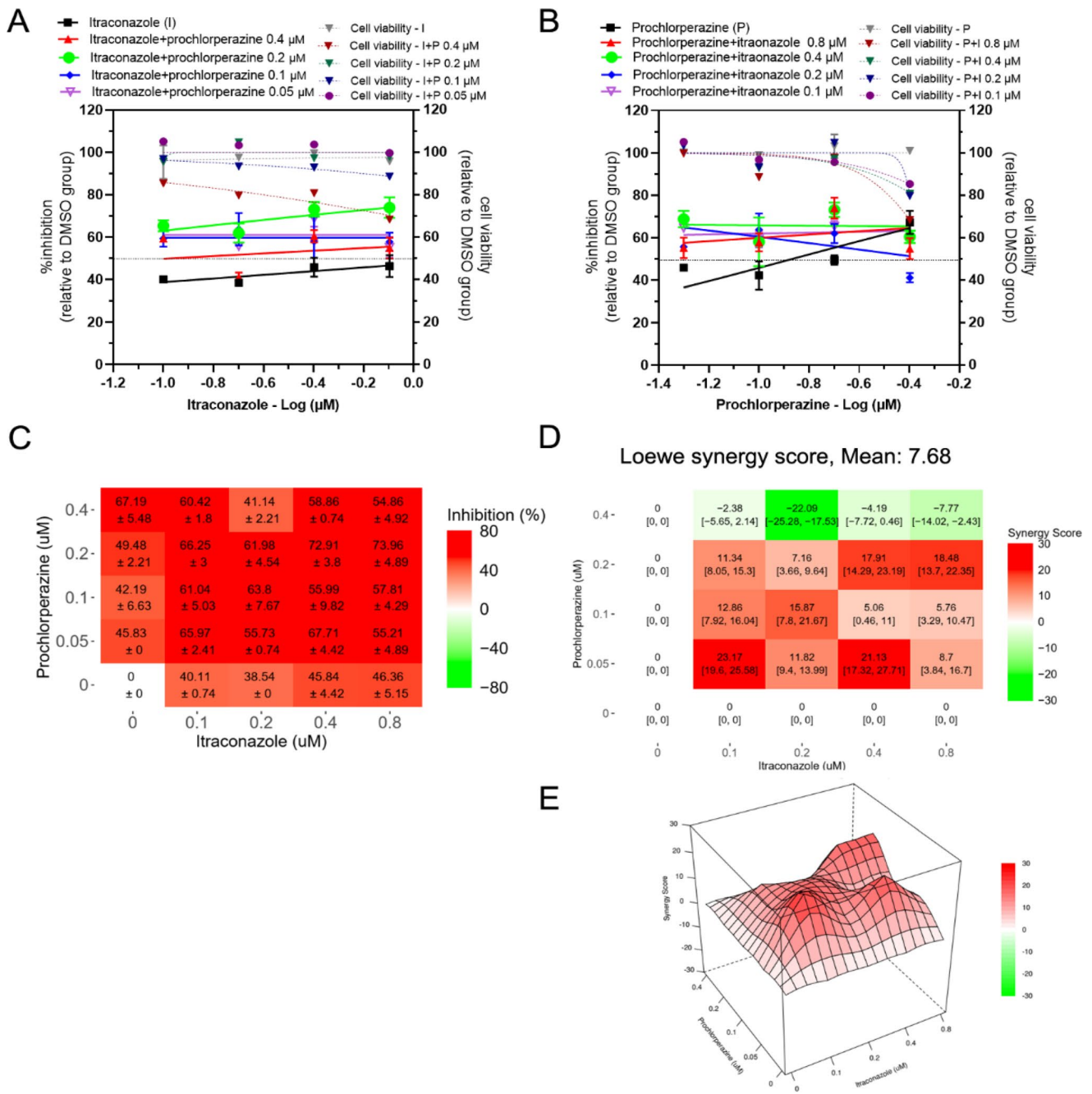
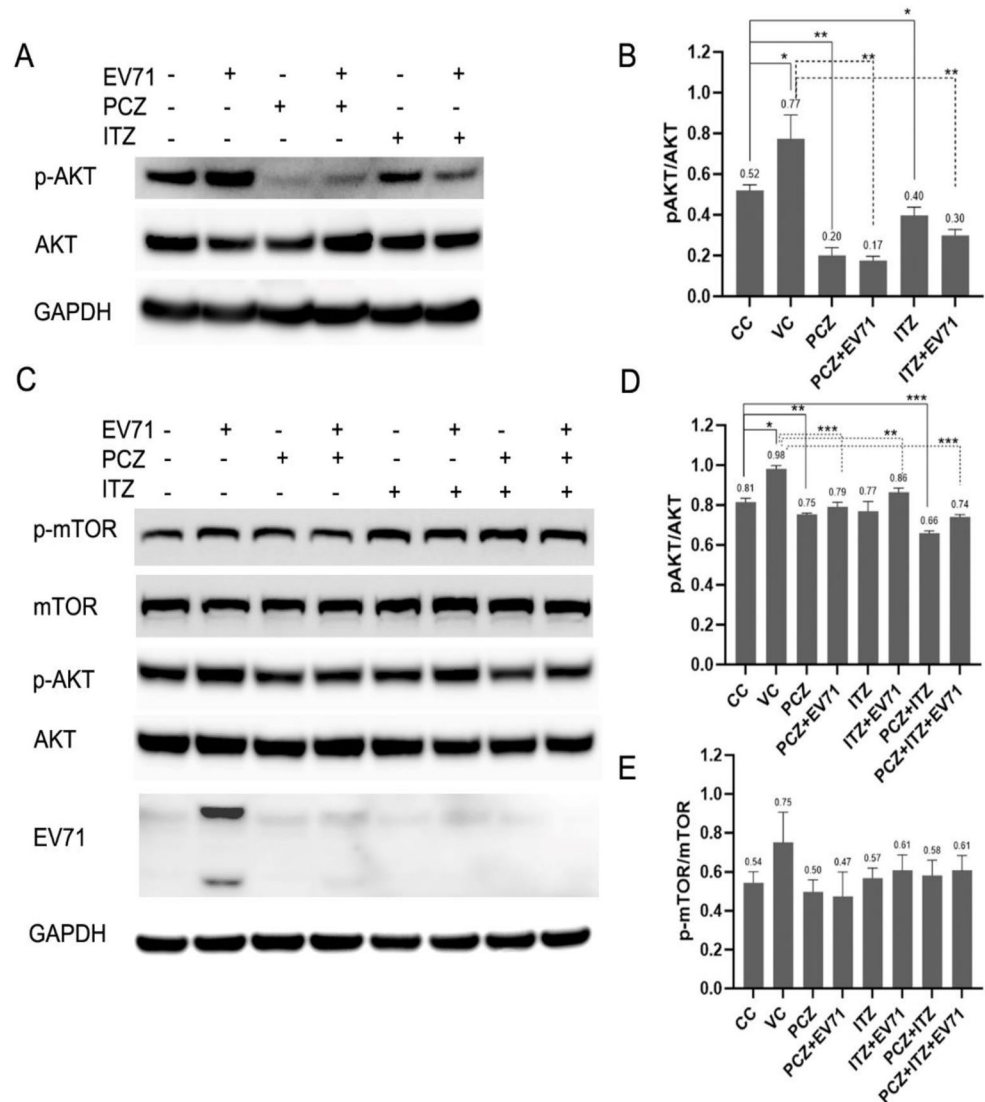


Fig. 7 Evaluation of the effect of itraconazole-prochlorperazine treatment on EV71 subgenotype C4 in neuroblastoma cells. Neuroblastoma cells (SH-SY5Y) were pretreated for 1 hour with 16 different pairwise combinations of different concentrations of itraconazole and prochlorperazine. The cells were then infected with EV71 subgenotype C4 at an MOI of 2. After removing the inoculum, the cells were maintained for two days in the medium containing drugs. Virus titers were determined using a plaque assay. The percent inhibition relative to 0.1%-DMSO-treated cells is shown in panel (A) for the treatment with twofold serial dilutions of itraconazole in the presence of different fixed concentrations of prochlorperazine and in panel (B) for the treat-

ment with twofold serial dilutions of prochlorperazine in the presence of different fixed concentrations of itraconazole. The dose-response matrix for each drug treatment is shown in panel (C). The data are presented as the mean ± standard deviation. The interaction between pairs of drugs was analyzed using SynergyFinder. The synergy score of each pairwise combination is presented as the mean and the confidence interval (D). A 3D synergy plot is shown in panel (E). A synergy score less than -10 indicates an antagonistic interaction between the two drugs; a score between -10 and 10 indicates an additive effect of the two drugs; and a score greater than 10 indicates a synergistic effect of the two drugs. I, itraconazole; P, prochlorperazine

Fig. 8 Western blot analysis of the effect of itraconazole and prochlorperazine treatment on EV71 subgenotype C4 infection in Vero and neuroblastoma cells. Vero or neuroblastoma (SH-SY5Y) cells were pretreated for 1 hour with prochlorperazine, itraconazole, a mixture of both drugs, or 0.1% DMSO. The cells were then infected with EV71 at an MOI of 1 and 2 for Vero and SH-SY-5Y cells, respectively. After removing the inoculum, the cells were maintained in the medium containing drugs for 1 hour (Vero) or 24 hours (SH-SY5Y). The infected cells were then collected and subjected to western blot analysis. **(A)** Vero cells. **(C)** SH-SY5Y cells. The intensities of the protein bands were quantitated, and the relative expression was determined for Vero cells **(B)** and SH-SY5Y cells **(D, E)**. The data are shown as the mean \pm standard deviation (*, $p \leq 0.05$; **, $p \leq 0.01$; ***, $p \leq 0.001$). PCZ, prochlorperazine; ITZ, itraconazole; (-), absent; (+), present



with the reduced level of EV71 replication in neuroblastoma cells.

Discussion

Viruses require cellular machinery of the host in every step of their replication. Therefore, these factors are potential targets of antiviral agents with broad antiviral activity. Recently, several studies demonstrated the antiviral activity of FDA-approved drugs through repurposed drug screenings. Many repurposed drugs showed broad-spectrum antiviral activity, targeting host cellular factors. Moreover, the use of repurposed drugs also expedites antiviral development due to their known safety profiles and the availability of pharmacokinetic data. In this study, several repurposed drugs with broad-spectrum antiviral activity were screened for their antiviral activity against EV71. Three drugs

demonstrated antiviral activity against EV71, including prochlorperazine, niclosamide, and itraconazole. Itraconazole was reported previously to be a potent inhibitor of EV71 [53, 69]. Itraconazole was also found to inhibit other enteroviruses, including coxsackievirus A16, coxsackievirus B3, poliovirus 1, and enterovirus 68 [15, 53].

Upon infection, host cell factors are manipulated by viruses to create a favorable environment for viral replication. For entry of the virus, EV71 requires intact membrane cholesterol during endocytosis [35]. A previous study showed that lipid rafts are required for internalization of EV71 and are involved in activation of the PI3K/Akt signaling pathway in the early stage of infection [76]. It has been suggested that phosphorylation of PI3K/Akt signaling pathway components is a mechanism by which host cell apoptosis induced by EV71 infection is delayed [63, 70]. In particular, phosphorylation of Akt1 also activates mTOR,

resulting in increased cell proliferation, protein synthesis, and *de novo* fatty acid synthesis [71].

Itraconazole is a triazole that is used in antifungal treatment. It is known to decrease ergosterol synthesis, which is required for fungal cell membrane integrity, via the inhibition of 14 α -demethylase [40, 59]. In the early stage of enterovirus infection, Akt phosphorylation activates mTOR and its downstream products, resulting in increased lipid synthesis. Itraconazole decreases Akt activity, thus inhibiting Akt/mTOR signaling and downregulating lipogenic gene expression [71]. Furthermore, previous studies have demonstrated that itraconazole targets OSBP and OSBP-related protein 4 (ORP4), which are localized in enterovirus replication organelles and disrupt their function in cholesterol transport, thus inhibiting enterovirus replication [53]. Itraconazole also targets the viral NS3A protein, thus disrupting its function in PI4KB recruitment [15]. Our results showed a potent antiviral activity of itraconazole in both Vero cells and a neuroblastoma cell line, with a favorable selectivity index.

Prochlorperazine is a piperazine phenothiazine that is used to treat nausea, schizophrenia, migraines, and anxiety. Previous studies have demonstrated the antiviral activity of prochlorperazine in dengue virus (DENV), Zika virus (ZIKV), and hepatitis C virus (HCV) infections. This drug inhibits DENV infection by blocking viral binding via the D2 dopamine receptor and viral entry through clathrin-mediated endocytosis [21, 51]. Furthermore, a previous study showed that prochlorperazine can bind to the non-structural protein 3 (NS3) of DENV and ZIKV [49]. Prochlorperazine also inhibits HCV entry in the virus-host membrane fusion step by increasing the fluidity of the host membrane [6, 17]. Our study demonstrated potent *in vitro* anti-EV71 activity of prochlorperazine (Vero, IC₅₀ = 0.22 μ M; SH-SY5Y, IC₅₀ = 1.02 μ M). Prochlorperazine has been shown to interfere with Akt and mTORC1 activation, resulting in a decrease in proliferation signaling in cancer cells [4]. In this study, we demonstrated that prochlorperazine and itraconazole both inhibit EV71 infection through inhibition of Akt phosphorylation in the PI3K/Akt signaling pathway.

Niclosamide is an anthelmintic drug that is used to treat infestations of tapeworms. It is capable of regulating multiple cellular signaling pathways, including mTORC1, STAT3, NF- κ B, Notch, and Wnt/ β -catenin [9, 32, 65]. In several repurposed drug tests, niclosamide was shown to inhibit infection with several uses, including DENV [27], Japanese encephalitis virus (JEV) [12], HCV [36], Epstein-Barr virus (EBV) [23], HIV-1 [37], and SARS-CoV-2 [2, 24]. Niclosamide prevents DENV infection by inhibiting endosomal acidification and interfering with viral particle maturation [25, 27]. It also prevents mTORC1 activation, which inhibits EBV and HIV-1 [23, 37]. Our study

demonstrated that niclosamide can potentially inhibit EV71 (Vero, IC₅₀ = 0.125 μ M; SH-SY5Y, IC₅₀ = 0.29 μ M), which is consistent with a recent study on screening of antiviral compounds from an FDA-approved drug library [54]. EV71 has been shown to enter cells through pH-dependent endocytosis [35], and therefore, niclosamide possibly inhibits EV71 infection by blocking endosomal acidification, as was observed with DENV.

The combination of drugs is a strategy used to maximize drug efficiency and to minimize drug resistance by using drugs that act on different cellular targets or viral proteins. In this study, two-drug combinations were tested in Vero cells. Niclosamide and itraconazole showed the best synergistic antiviral activity against EV71. This two-drug combination reduced the IC₅₀ values of both drugs, suggesting that they are more effective when used in combination. The remaining combinations, niclosamide-prochlorperazine and itraconazole-prochlorperazine, showed additive effects. Both niclosamide and prochlorperazine inhibit endosomal acidification and mTOR activation, while both itraconazole and prochlorperazine inhibit the Akt/mTOR signaling pathway. These two-drug combinations act on the same cellular targets, resulting in additive rather than synergistic effects.

We also assessed the antiviral activity of two-drug combinations in neuroblastoma cells. However, niclosamide caused high cytotoxicity in this cell line, which is reflected in its unfavorable selectivity index of 1.34. Therefore, only the combination of itraconazole and prochlorperazine was tested in neuroblastoma cells, and this combination was found to have an additive effect.

In summary, we have identified prochlorperazine as a repurposed drug with antiviral activity against EV71. Importantly, prochlorperazine was also found to inhibit Akt phosphorylation in cells infected with EV71. The combination of niclosamide and itraconazole demonstrated a synergistic effect in Vero cells, but the combination of itraconazole and prochlorperazine showed only an additive effect in Vero and neuroblastoma cells. Different antiviral activities of these drugs, either alone or in combination, were observed in different cell lines. Thus, they still need to be evaluated in animal models. Our results indicate that it is feasible to develop therapeutic treatments of EV71 infection using repurposed drugs, alone or in two-drug combinations.

Acknowledgments This study was supported by the National Research Council of Thailand and the Faculty of Medicine of Siriraj Hospital, Mahidol University, Thailand (SI-09/2562). We thank Prof. Pilaipan Puthavathana for kindly providing the virus.

Author contributions Kunlakanya Jitobaom conducted a drug treatment experiment, viral quantification, and data analysis and was a major contributor in the writing of the manuscript. Chompunuch Boonarkart performed viral quantification and optimization of infection methods. Songkran Thongon and Thanyporn Sirihongthong prepared

viral stocks and optimized the plaque assay for EV71. Arpakorn Sornwong performed viral quantification. Prasert Auewarakul reviewed and edited the manuscript. Ormpreya Suptawiwat designed and supervised the study, acquired funding, and reviewed and edited the manuscript. All authors read and approved the final manuscript.

Funding This study was supported by the National Research Council of Thailand and the Faculty of Medicine of Siriraj Hospital, Mahidol University, Thailand (SI-09/2562). The funders had no role in study design, data collection, analysis, or interpretation or in writing the manuscript.

Data availability The datasets generated and/or analyzed in the current study are available from the corresponding author on reasonable request.

Declarations

Ethical approval This article does not contain any studies with human participants or animals performed by any of the authors.

Conflict of interest The authors have no relevant financial or non-financial interests to disclose.

References

1. AASLD (2021) HCV Guidance: Recommendations for testing, managing, and treating Hepatitis C Virus infection. Infectious Diseases Society of America
2. Backer V, Sjöbring U, Sonne J, Weiss A, Hostrup M, Johansen HK, Becker V, Sonne DP, Balchen T, Jellingsø M, Sommer MOA (2021) A randomized, double-blind, placebo-controlled phase 1 trial of inhaled and intranasal niclosamide: A broad spectrum antiviral candidate for treatment of COVID-19. *Lancet Reg Health Eur* 4:100084
3. Barrows NJ, Campos RK, Powell ST, Prasanth KR, Schott-Lerner G, Soto-Acosta R, Galarza-Muñoz G, McGrath EL, Urrabaz-Garza R, Gao J, Wu P, Menon R, Saade G, Fernandez-Salas I, Rossi SL, Vasilakis N, Routh A, Bradrick SS, Garcia-Blanco MA (2016) A screen of FDA-approved drugs for inhibitors of Zika virus infection. *Cell Host Microbe* 20:259–270
4. Bonnet R, Nebout M, Brousse C, Reinier F, Imbert V, Rohrlisch PS, Peyron J-F (2020) New Drug Repositioning Candidates for T-ALL Identified Via Human/Murine Gene Signature Comparison. 10
5. Cabrerizo M, Tarragó D, Muñoz-Almagro C, del Amo E, Domínguez-Gil M, Eiros JM, López-Miragaya I, Pérez C, Reina J, Otero A, González I, Echevarría JE, Trallero G (2014) Molecular epidemiology of enterovirus 71, coxsackievirus A16 and A6 associated with hand, foot and mouth disease in Spain. *Clin Microbiol Infect* 20:O150–O156
6. Chamoun-Emanuelli AM, Pecheur E-I, Simeon RL, Huang D, Cremer PS, Chen Z (2013) Phenothiazines inhibit hepatitis C virus entry, likely by increasing the fluidity of cholesterol-rich membranes. *Antimicrob Agents Chemother* 57:2571–2581
7. Chen M, Ju Y, Chen M, Xie Z, Zhou K, Tan Y, Mo J (2017) Epidemiological and genetic characteristics of EV71 in hand, foot, and mouth disease in Guangxi, southern China, from 2010 to 2015. *PLoS ONE* 12:e0188640
8. Chen Y, Gu F, Guan J-L (2018) Metformin Might Inhibit Virus through Increasing Insulin Sensitivity. *Chin Med J* 131:376–377
9. Cheng B, Morales LD, Zhang Y, Mito S, Tsin A (2017) Niclosamide induces protein ubiquitination and inhibits multiple pro-survival signaling pathways in the human glioblastoma U-87 MG cell line. *PLoS ONE* 12:e0184324–e0184324
10. Cho J, Yi H, Jang EY, Lee MS, Lee JY, Kang C, Lee CH, Kim K (2017) Mycophenolic mofetil, an alternative antiviral and immunomodulator for the highly pathogenic avian influenza H5N1 virus infection. *Biochem Biophys Res Commun* 494:298–304
11. Coll B, van Wijk JP, Parra S, Castro Cabezas M, Hoepelman IM, Alonso-Villaverde C, de Koning EJ, Camps J, Ferre N, Rabelink TJ, Tous M, Joven J (2006) Effects of rosiglitazone and metformin on postprandial paraoxonase-1 and monocyte chemoattractant protein-1 in human immunodeficiency virus-infected patients with lipodystrophy. *Eur J Pharmacol* 544:104–110
12. Fang J, Sun L, Peng G, Xu J, Zhou R, Cao S, Chen H, Song Y (2013) Identification of three antiviral inhibitors against Japanese encephalitis virus from library of pharmacologically active compounds 1280. *PLoS ONE* 8:e78425
13. Fraser JE, Watanabe S, Wang C, Chan WK, Maher B, Lopez-Denman A, Hick C, Wagstaff KM, Mackenzie JM, Sexton PM, Vasudevan SG, Jans DA (2014) A nuclear transport inhibitor that modulates the unfolded protein response and provides in vivo protection against lethal dengue virus infection. *J Infect Dis* 210:1780–1791
14. Friedman BW, Irizarry E, Solorzano C, Latev A, Rosa K, Zias E, Vinson DR, Bijur PE, Gallagher EJ (2017) Randomized study of IV prochlorperazine plus diphenhydramine vs IV hydromorphone for migraine. *Neurology* 89:2075–2082
15. Gao Q, Yuan S, Zhang C, Wang Y, Wang Y, He G, Zhang S, Altmeyer R, Zou G (2015) Discovery of Itraconazole with broad-spectrum *in vitro* antienterovirus activity that targets nonstructural protein 3A. 59:2654–2665
16. García-Serradilla M, Risco C, Pacheco B (2019) Drug repurposing for new, efficient, broad spectrum antivirals. *Virus Res* 264:22–31
17. Gastaminza P, Whitten-Bauer C, Chisari FV (2010) Unbiased probing of the entire hepatitis C virus life cycle identifies clinical compounds that target multiple aspects of the infection. *Proc Natl Acad Sci U S A* 107:291–296
18. Hart BJ, Dyall J, Postnikova E, Zhou H, Kindrachuk J, Johnson RF, Olinger GG, Frieman MB, Holbrook MR, Jahrling PB, Hensley L (2014) Interferon- β and mycophenolic acid are potent inhibitors of Middle East respiratory syndrome coronavirus in cell-based assays. *J Gen Virol* 95:571–577
19. Hewitt RG, Yiannoutsos CT, Higgs ES, Carey JT, Geiseler PJ, Soave R, Rosenberg R, Vazquez GJ, Wheat LJ, Fass RJ, Antoninovic Z, Walawander AL, Flanigan TP, Bender JF (2000) Paromomycin: no more effective than placebo for treatment of cryptosporidiosis in patients with advanced human immunodeficiency virus infection. AIDS Clinical Trial Group. *Clin Infect Dis* 31:1084–1092
20. Hickson SE, Margineantu D, Hockenbery DM, Simon JA, Geballe AP (2018) Inhibition of vaccinia virus replication by nitazoxanide. *Virology* 518:398–405
21. Ho M-R, Tsai T-T, Chen C-L, Jhan M-K, Tsai C-C, Lee Y-C, Chen C-H, Lin C-F (2017) Blockade of dengue virus infection and viral cytotoxicity in neuronal cells *in vitro* and *in vivo* by targeting endocytic pathways. *Sci Rep* 7:6910
22. Hong J, Liu F, Qi H, Tu W, Ward MP, Ren M, Zhao Z, Su Q, Huang J, Chen X, Le J, Ren X, Hu Y, Cowling B, Li Z, Chang Z, Zhang Z (2022) Changing epidemiology of hand, foot, and mouth disease in China, 2013–2019: a population-based study. *The Lancet Regional Health – Western Pacific* 20
23. Huang L, Yang M, Yuan Y, Li X, Kuang E (2017) Niclosamide inhibits lytic replication of Epstein-Barr virus by disrupting mTOR activation. *Antiviral Res* 138:68–78
24. Jeon S, Ko M, Lee J, Choi I, Byun SY, Park S, Shum D, Kim S (2020) Identification of Antiviral Drug Candidates against

- SARS-CoV-2 from FDA-Approved Drugs. *Antimicrob Agents Chemother* 64
25. Jung E, Nam S, Oh H, Jun S, Ro HJ, Kim B, Kim M, Go YY (2019) Neutralization of Acidic Intracellular Vesicles by Niclosamide Inhibits Multiple Steps of the Dengue Virus Life Cycle *In Vitro*. *Sci Rep* 9:8682
 26. Jurgeit A, McDowell R, Moese S, Meldrum E, Schwendener R, Greber UF (2012) Niclosamide is a proton carrier and targets acidic endosomes with broad antiviral effects. *PLoS Pathog* 8:e1002976
 27. Kao J-C, HuangFu W-C, Tsai T-T, Ho M-R, Jhan M-K, Shen T-J, Tseng P-C, Wang Y-T, Lin C-F (2018) The antiparasitic drug niclosamide inhibits dengue virus infection by interfering with endosomal acidification independent of mTOR. *PLOS Negl Trop Dis* 12:e0006715–e0006715
 28. Kuo R-L, Shih S-R (2013) Strategies to develop antivirals against enterovirus 71. *Virology* 453:28–38
 29. Lee KY (2016) Enterovirus 71 infection and neurological complications. *Korean J Pediatr* 59:395–401
 30. Lei D, Griffiths E, Martin J (2020) WHO working group meeting to develop WHO Recommendations to assure the quality, safety and efficacy of enterovirus 71 vaccines. *Vaccine* 38:4917–4923
 31. Li X, Peng T (2021) Strategy, progress, and challenges of drug repurposing for efficient antiviral discovery. *Front Pharmacol* 12
 32. Li Y, Li PK, Roberts MJ, Arend RC, Samant RS, Buchsbaum DJ (2014) Multi-targeted therapy of cancer by niclosamide: A new application for an old drug. *Cancer Lett* 349:8–14
 33. Li Z, Brecher M, Deng YQ, Zhang J, Sakamuru S, Liu B, Huang R, Koetzner CA, Allen CA, Jones SA, Chen H, Zhang NN, Tian M, Gao F, Lin Q, Banavali N, Zhou J, Boles N, Xia M, Kramer LD, Qin CF, Li H (2017) Existing drugs as broad-spectrum and potent inhibitors for Zika virus by targeting NS2B-NS3 interaction. *Cell Res* 27:1046–1064
 34. Lin J-Y, Kung Y-A, Shih S-R (2019) Antivirals and vaccines for Enterovirus A71. *J Biomed Sci* 26:65
 35. Lin Y-W, Lin H-Y, Tsou Y-L, Chitra E, Hsiao K-N, Shao H-Y, Liu C-C, Sia C, Chong P, Chow Y-H (2012) Human SCARB2-mediated entry and endocytosis of EV71. *PLoS ONE* 7:e30507–e30507
 36. Mazzoni M, Ortega-Prieto AM, Imrie D, Luft C, Hess L, Czieso S, Grove J, Skelton JK, Farleigh L, Bugert JJ, Wright E, Temperton N, Angell R, Oxenford S, Jacobs M, Ketteler R, Dorner M, Marsh M (2019) Identification of broad-spectrum antiviral compounds by targeting viral entry. *Viruses* 11:176
 37. Niyomdechana N, Suptawiwat O, Boonarkart C, Jitobaom K, Auevarakul P (2020) Inhibition of human immunodeficiency virus type 1 by niclosamide through mTORC1 inhibition. *Heliyon* 6:e04050–e04050
 38. Noisumdaeng P, Sangsiriwut K, Prasertsopon J, Klinmalai C, Payungporn S, Mungaomklang A, Choekhaibulkit K, Buathong R, Thithithayanont A, Puthavathana P (2018) Complete genome analysis demonstrates multiple introductions of enterovirus 71 and coxsackievirus A16 recombinant strains into Thailand during the past decade. *Emerg Microbes Infect* 7:214
 39. Otreba M, Kosmider L (2021) In vitro anticancer activity of fluphenazine, perphenazine and prochlorperazine. A review. *J Appl Toxicol* 41:82–94
 40. Pantziarka Pan SV, Bouche Gauthier M, Lydie, Sukhatme Vikas P (2015) Repurposing Drugs in Oncology (ReDO)—itraconazole as an anti-cancer agent. *ecancer* 9
 41. Paplomata E, O'Regan R (2014) The PI3K/AKT/mTOR pathway in breast cancer: targets, trials and biomarkers. *Ther Adv Med Oncol* 6:154–166
 42. Perelygina L, Hautala T, Seppänen M, Adebayo A, Sullivan KE, Icenogle J (2017) Inhibition of rubella virus replication by the broad-spectrum drug nitazoxanide in cell culture and in a patient with a primary immune deficiency. *Antiviral Res* 147:58–66
 43. Phougat N, Khatri S, Singh A, Dangi M, Kumar M, Dabur R, Chhillar AK (2014) Combination therapy: the propitious rationale for drug development. *Comb Chem High Throughput Screen* 17:53–67
 44. Puenpa J, Wanlapakorn N, Vongpunsawad S, Poovorawan Y (2019) The History of Enterovirus A71 Outbreaks and Molecular Epidemiology in the Asia-Pacific Region. *J Biomed Sci* 26:75
 45. Romero-Gómez M, Diago M, Andrade RJ, Calleja JL, Salmerón J, Fernández-Rodríguez CM, Solà R, García-Samaniego J, Hererías JM, De la Mata M, Moreno-Otero R, Nuñez O, Olveira A, Durán S, Planas R (2009) Treatment of insulin resistance with metformin in naïve genotype 1 chronic hepatitis C patients receiving peginterferon alfa-2a plus ribavirin. *Hepatology* 50:1702–1708
 46. Rossignol JF (2014) Nitazoxanide: a first-in-class broad-spectrum antiviral agent. *Antiviral Res* 110:94–103
 47. Rossignol JF (2016) Nitazoxanide, a new drug candidate for the treatment of Middle East respiratory syndrome coronavirus. *J Infect Public Health* 9:227–230
 48. Sacramento CQ, de Melo GR, de Freitas CS, Rocha N, Hoelz LV, Miranda M, Fintelman-Rodrigues N, Marttorelli A, Ferreira AC, Barbosa-Lima G, Abrantes JL, Vieira YR, Bastos MM, de Mello Volotão E, Nunes EP, Tschoeke DA, Leomil L, Loiola EC, Trindade P, Rehen SK, Bozza FA, Bozza PT, Boechat N, Thompson FL, de Filippis AM, Brüning K, Souza TM (2017) The clinically approved antiviral drug sofosbuvir inhibits Zika virus replication. *Sci Rep* 7:40920
 49. Sahoo M, Jena L, Daf S, Kumar S (2016) Virtual Screening for Potential Inhibitors of NS3 Protein of Zika Virus. *Genomics Inf* 14:104–111
 50. Shi Z, Wei J, Deng X, Li S, Qiu Y, Shao D, Li B, Zhang K, Xue F, Wang X, Ma Z (2014) Nitazoxanide inhibits the replication of Japanese encephalitis virus in cultured cells and in a mouse model. *Virology* 461:11–19
 51. Simanjuntak Y, Liang JJ, Lee YL, Lin YL (2015) Repurposing of prochlorperazine for use against dengue virus infection. *J Infect Dis* 211:394–404
 52. Solomon T, Lewthwaite P, Perera D, Cardoso MJ, McMinn P, Ooi MH (2010) Virology, epidemiology, pathogenesis, and control of enterovirus 71. *Lancet Infect Dis* 10:778–790
 53. Strating JRPM, van der Linden L, Albuilescu L, Bigay J, Arita M, Delang L, Leysen P, van der Schaar HM, Lanke KHW, Thibaut HJ, Ulferts R, Drin G, Schlinck N, Wubbolts RW, Sever N, Head SA, Liu JO, Beachy PA, De Matteis MA, Shair MD, Olkkonen VM, Neyts J, van Kuppeveld FJM (2015) Itraconazole inhibits enterovirus replication by targeting the oxysterol-binding protein. *Cell Rep* 10:600–615
 54. Sun J, Yogarajah T, Lee RCH, Kaur P, Inoue M, Tan YW, Chu JH (2020) Drug repurposing of pyrimidine analogs as potent antiviral compounds against human enterovirus A71 infection with potential clinical applications. *Sci Rep* 10:8159
 55. Takatsuki A, Tamura G, Arima K (1969) Antiviral and Antitumor Antibiotics. XIV. Effects of Ascochlorin and Other Respiration Inhibitors on Multiplication of Newcastle Disease Virus in Cultured Cells. *J Biol Chem* 244:825–829
 56. Tariq A, Mateen RM, Afzal MS, Saleem M (2020) Paromomycin: A potential dual targeted drug effectively inhibits both spike (S1) and main protease of COVID-19. *Int J Infect Dis* 98:166–175
 57. Thammasonthijarern N, Kosoltanapiwat N, Nuprasert W, Sitikul P, Sriburin P, Pan-ngum W, Maneekan P, Hataiyusuk S, Hattasingh W, Thaipadungpanit J, Chatchen S (2021) Molecular Epidemiological Study of Hand, Foot, and Mouth Disease in a Kindergarten-Based Setting in Bangkok. *Thail Pathogens* 10:576
 58. Tsubamoto H, Inoue K, Sakata K, Ueda T, Takeyama R, Shibahara H, Sonoda T (2017) Itraconazole Inhibits AKT/mTOR Signaling

- and Proliferation in Endometrial Cancer Cells. *Anticancer Res* 37:515–519
59. Vanden Bossche H, Marichal P, Le Jeune L, Coene MC, Goren J, Cools W (1993) Effects of itraconazole on cytochrome P-450-dependent sterol 14 alpha-demethylation and reduction of 3-ketosteroids in *Cryptococcus neoformans*. *Antimicrob Agents Chemother* 37:2101–2105
 60. Wang J, Hu Y, Zheng M (2022) Enterovirus A71 antivirals: Past, present, and future. *Acta Pharm Sin B* 12:1542–1566
 61. Wang YM, Lu JW, Lin CC, Chin YF, Wu TY, Lin LI, Lai ZZ, Kuo SC, Ho YJ (2016) Antiviral activities of niclosamide and nitazoxanide against chikungunya virus entry and transmission. *Antiviral Res* 135:81–90
 62. WHO (2018) Updated recommendations on first-line and second-line antiretroviral regimens and post-exposure prophylaxis and recommendations on early infant diagnosis of HIV
 63. Wong WR, Chen YY, Yang SM, Chen YL, Horng JT (2005) Phosphorylation of PI3K/Akt and MAPK/ERK in an early entry step of enterovirus 71. *Life Sci* 78:82–90
 64. Wu CJ, Jan JT, Chen CM, Hsieh HP, Hwang DR, Liu HW, Liu CY, Huang HW, Chen SC, Hong CF, Lin RK, Chao YS, Hsu JT (2004) Inhibition of severe acute respiratory syndrome coronavirus replication by niclosamide. *Antimicrob Agents Chemother* 48:2693–2696
 65. Xu J, Shi P-Y, Li H, Zhou J (2020) Broad Spectrum Antiviral Agent Niclosamide and Its Therapeutic Potential. *ACS Infect Dis* 6:909–915
 66. Xun YH, Zhang YJ, Pan QC, Mao RC, Qin YL, Liu HY, Zhang YM, Yu YS, Tang ZH, Lu MJ, Zang GQ, Zhang JM (2014) Metformin inhibits hepatitis B virus protein production and replication in human hepatoma cells. *J Viral Hepat* 21:597–603
 67. Yadav B, Wennerberg K, Aittokallio T, Tang J (2015) Searching for drug synergy in complex dose–response landscapes using an interaction potency model. *Comput Struct Biotechnol* 13:504–513
 68. Yi L, Lu J, Kung HF, He ML (2011) The virology and developments toward control of human enterovirus 71. *Crit Rev Microbiol* 37:313–327
 69. Zeng S, Meng X, Huang Q, Lei N, Zeng L, Jiang X, Guo X (2019) Spiramycin and azithromycin, safe for administration to children, exert antiviral activity against enterovirus A71 in vitro and in vivo. *Int J Antimicrob Agents* 53:362–369
 70. Zhang H, Li F, Pan Z, Wu Z, Wang Y, Cui Y (2014) Activation of PI3K/Akt pathway limits JNK-mediated apoptosis during EV71 infection. *Virus Res* 192:74–84
 71. Zhang T, Huang J, Yi Y, Zhang X, Loo JJ, Cao Y, Shi H, Luo J (2018) Akt Serine/Threonine Kinase 1 Regulates de Novo Fatty Acid Synthesis through the Mammalian Target of Rapamycin/Sterol Regulatory Element Binding Protein 1 Axis in Dairy Goat Mammary Epithelial Cells. *J Agric Food Chem* 66:1197–1205
 72. Zhang W, Bhagwath AS, Ramzan Z, Williams TA, Subramanian I, Edpuganti V, Kallem RR, Dunbar KB, Ding P, Gong K, Geurkink SA, Beg MS, Kim J, Zhang Q, Habib AA, Choi SH, Lapsiwala R, Bhagwath G, Dowell JE, Melton SD, Jie C, Putnam WC, Pham TH, Wang DH (2021) Itraconazole Exerts Its Antitumor Effect in Esophageal Cancer By Suppressing the HER2/AKT Signaling Pathway. *Mol Cancer Ther* 20:1904–1915
 73. Zhang X-N, Song Z-G, Jiang T, Shi B-S, Hu Y-W, Yuan Z-H (2010) Rupintrivir is a promising candidate for treating severe cases of Enterovirus-71 infection. *World J Gastroenterol* 16:201–209
 74. Zhang Y, Han H, Sun L, Qiu H, Lin H, Yu L, Zhu W, Qi J, Yang R, Pang Y, Wang X, Lu G, Yang Y (2017) Antiviral activity of shikonin ester derivative PMM-034 against enterovirus 71 in vitro. *Braz J Med Biol Res* 50:e6586
 75. Zhao Q, Xiong Y, Xu J, Chen S, Li P, Huang Y, Wang Y, Chen W-X, Wang B (2018) Host MicroRNA hsa-miR-494-3p Promotes EV71 Replication by Directly Targeting PTEN. *Frontiers in Cellular and Infection Microbiology* 8
 76. Zhu YZ, Wu DG, Ren H, Xu QQ, Zheng KC, Chen W, Chen SL, Qian XJ, Tao QY, Wang Y, Zhao P, Qi ZT (2015) The Role of Lipid Rafts in the Early Stage of Enterovirus 71 Infection. *Cell Physiol Biochem* 35:1347–1359

Publisher's Note Springer Nature remains neutral with regard to jurisdictional claims in published maps and institutional affiliations.

Springer Nature or its licensor (e.g. a society or other partner) holds exclusive rights to this article under a publishing agreement with the author(s) or other rightsholder(s); author self-archiving of the accepted manuscript version of this article is solely governed by the terms of such publishing agreement and applicable law.